FFI Norwegian Defence Research Establishment

23/01769

FFI-RAPPORT

Literature review of atmospheric contaminant transport offshore

Espen Åkervik
Thor Gjesdal

Literature review of atmospheric contaminant transport offshore

Espen Åkervik
Thor Gjesdal

Norwegian Defence Research Establishment (FFI) 17 November 2023

Keywords
Turbulens
Bølger
Computational Fluid Dynamics (CFD)

FFI report
23/01769

Project number
1575

Electronic ISBN
978-82-464-3509-1

Approvers
Janet M. Blatny, *Director of Research*
Anders Helgeland, *Research Manager*

The document is electronically approved and therefore has no handwritten signature.

Summary

In this report, we consider the atmospheric dispersion of possibly harmful contaminants from offshore accidents by doing a literature review on the subject.

The atmospheric dispersion is mainly governed by the wind, which exhibits chaotic behaviour due the interplay of large-scale circulation patterns and surface conditions. An operational model needs to be fast and easy to use. This can be achieved by avoiding to describe the wind conditions in detail. The so called Gaussian models are arguably the most well known examples of such simplified models. If the winds are steady and flow over relatively flat terrain, these models may give realistic estimates of the dispersion. However, if the wind is perturbed by buildings and topography, or if the contaminants are transported over long distances, such simple models are bound to fall short. In such cases, we need a model that can utilise wind input with a higher complexity, either in the form of turbulence resolving models or numerical weather prediction models.

Wind flow over sea has traditionally been considered as simpler than wind flow over land surfaces, and ocean waves have been considered as mild roughness elements that lead to low turbulence levels. While it is true that offshore wind turbulence levels are low compared to onshore turbulence levels, research has shown that there is a complex relation between the sea state and the vertical transport mechanism. The sea state refers to whether the waves are short (and slow) or long (and fast). Short waves always travel in the direction of the wind, and their effect is a net momentum transfer downwards that ultimately slows down the wind while the waves grow. Long waves, on the other hand, commonly referred to as swell waves, can travel in any direction. If these long waves travel in the direction of the wind, they provide thrust to the wind while decaying. Conversely, if they travel counter to the direction of the wind, they slow down the wind while decaying. This complex relation between sea state and the energy transfer between the sea and air, raises the question of how atmospheric dispersion is affected by the interaction between the wind and the waves.

In our literature review, we found only a limited number of references that address this topic. In these references we found the following:

- Multiple references agree that swell waves travelling in the same direction as the wind lead to enhanced suspension of aerosols. This means that aerosols are transported upward, away from the surface, thus counteracting deposition and consequently leading to higher concentrations downstream of the source.
- A single reference, in which numerical calculations were performed on a laboratory scale, showed that short waves lead to enhanced deposition of aerosols.

Our main impression is, however, that there is a lack of literature on this topic.

Recently, a class of flow models known as wall-modelled large eddy simulation models (LES) has been adopted to, and tested on, the flow over waves on operational scales. These models represent, in our opinion, the most promising candidate to investigate the effect of waves on dispersion of pollutants close to the sea surface.

Sammendrag

I denne rapporten er vi opptatt av atmosfærisk spredning av mulige skadelige stoffer fra offshoreulykker, og vi ser på hva som finnes av forskningslitteratur som er relevant for å modellere dette.

Den atmosfæriske spredningen er først og fremst styrt av vinden, som utviser kaotisk oppførsel på grunn av samspillet mellom storskala sirkulasjonsmønstre og overflateforhold. En operasjonell modell for spredningen trenger å være rask og enkel å bruke. Dette kan man oppnå ved å la være å beskrive vindforholdene for detaljert. Den såkalte Gauss-modellen er den mest kjente av slike modeller. Dersom vinden er jevn og dersom det er lite terrengvariasjon, kan slike modeller fungere godt. Men når vinden påvirkes av bygninger og topografi, eller dersom man står overfor transport over lange avstander, er disse enkle modellene nesten garantert å komme til kort. I slike tilfeller må vi heller ty til modeller som kan utnytte mer kompleks vind i form av turbulensmodeller eller numeriske værprediksjonsmodeller.

Vind over hav har tradisjonelt blitt sett på som enklere enn vind over land, og havbølgene har blitt sett på som milde ruhetselementer som fører til lave turbulensnivåer. Selv om turbulensnivåer over hav er lave sammenlignet med over land, har forskning vist at det er en kompleks sammenheng mellom sjøtilstanden og den vertikale transportmekanismen. Sjøtilstanden handler om hvorvidt bølgene er korte (og sakte) eller lange (og raske). Korte bølger forplanter seg utelukkende i retning av vinden, og effekten av dem er en netto overføring av energi til bølgene, med den effekten at bølgene vokser mens vinden blir bremset. Lange bølger derimot, ofte referert til som dønninger, kan forplante seg i alle retninger. Hvis disse lange bølgene forplanter seg i vindens retning, vil de gi en netto skyvekraft til vinden samtidig som de sakte avtar i høyde. Dersom de derimot forplanter seg mot vinden, vil de bremse vinden. Denne komplekse sammenhengen mellom sjøtilstand og overføring av energi mellom hav og atmosfære, reiser spørsmålet om hvordan den atmosfæriske spredningen blir påvirket av samspillet mellom vind og bølger.

I gjennomgangen vår fant vi bare en håndfull referanser som tar for seg dette emnet. I disse fant vi følgende:

- Flere referanser er enige om at dønninger som forplanter seg i samme retning som vinden, fører til at aerosoler transporteres oppover, vekk fra overflaten. Dønninger motvirker altså avsetning på overflaten, noe som fører til høyere luftkonsentrasjoner nedstrøms for kilden.
- Én av referansene, der forskeren hadde utført numeriske beregninger på laboratorieskala, viste at korte bølger fører til økt avsetning av aerosoler på overflaten.

Hovedinntrykket er imidlertid at det er stor mangel på litteratur på dette emnet. Nylig har såkalte veggmodellerte LES modeller (LES, eng. for large eddy simulation) blitt tatt i bruk for og testet på vind over bølger på operativ skala, altså på domener som strekker seg over flere kilometer. Disse modellene representerer, etter vår mening, den mest lovende kandidaten til å undersøke effekten av bølger på spredning av utslipp nær havoverflaten.

Contents

1 Introduction

Modeling of the release and transport of pollutants, also referred to as dispersion modeling, is an integral part of public crisis management. Released contaminants, in the form of biological, chemical, or radiological agents, are transported away from the source in air (and/or water), and may pose a threat to lives and to the environment. In this report, we review the modeling of contaminant transport in air for offshore conditions. This is especially relevant in the context of offshore accidents that lead to emission of harmful substances.

The key elements in order to quantify the impact of pollution events are: i) Description of the pollution source, including the type and amount of pollutant as well as the type and duration of the release, ii) the transport of the pollutant with the wind, and (iii) the impact of the dispersed pollutant on humans, animals and the environment. While all three points are important, our focus is on the transport mechanisms in air. These transport mechanisms contain many sub-processes such as turbulent transport, rainout, dry deposition, clustering, fragmentation, and radioactive decay. Our primary aim is to discuss the differences between contaminant transport in the atmosphere over sea (offshore) and over land (onshore). We will therefore focus on how the wind field, including diffusion processes, differ in these two cases.

For onshore conditions, the complexity of the wind field increases with complexity in topography, and winds in urban or mountainous regions are to a large extent dictated by the geometry (Britter and Hanna, 2003). For mild topography changes, the wind fields may be described by simple analytical formulas such as the log law (Stull, 1988), in which the effect of vegetation and mild topography changes can be parameterized by a roughness length. As the geometry becomes more complex, a more sophisticated modeling approach is needed (Boris et al., 2004). The heat fluxes caused by from the differences in air and ground temperatures, depend strongly on insolation and the specific type of sub-surface (ranging from asphalt to snow), and ranges from strong vertical mixing by convection if the ground is hotter than the air to complete damping of turbulence if the ground is colder than the air.

Offshore conditions are, in some respects, less complicated than onshore conditions since the topography is simple, from a macroscopic point of view, leading to relatively low turbulence levels and less aerodynamic drag from the surface. Furthermore, smaller temperature variation is present (Joshi et al., 2008) since oceans have altered hydrological cycles compared to land. On the other hand, the modeling of wind over waves is complicated by the fact that the air-sea interface is a dynamic surface, at which the conditions are governed by a spectrum of waves traveling at different speeds (Hasselmann et al., 1973; Janssen, 2004). The waves are generated by winds by a process that is only partly understood (Miles, 1962; Belcher and Hunt, 1998). The drag provided by waves is difficult to model properly because of the non-obvious way that the dynamics of the system depend on the ratio of the wind speed and the wave speed (Sullivan and McWilliams, 2010). The problem of the wind-wave interactions is characterized by scale separation between the large turbulent eddies in the atmosphere and the small adjustment zone where the wave induced perturbations adjust to the atmospheric flow. Furthermore, it is difficult to perform accurate measurements close to the undulating surface. Because of these issues, it is difficult to draw definite conclusions on the characteristics of wind wave interactions.

Dispersion models can broadly be put into two categories; models that rely on very simple wind description and models that rely on detailed wind description. The most well known models based

on simple wind description is the class of Gaussian plume models (Hanna et al., 1982), in which only estimates of wind direction, wind speed and turbulence levels are needed. The models that rely on detailed wind information may use any flow model, including computational fluid dynamics models on small spatial scales, see e.g. (Versteeg and Malalasekera, 2007), or numerical weather prediction models on larger spatial scales, e.g. (Warner, 2010; Bauer et al., 2015). These detailed models typically represent the dispersion either as a concentration field (Eulerian description) or as individual particles/particle packets (Lagrangian description). See Britter and Hanna (2003) for an in-depth discussion of these modeling options.

Hanna et al. (1985) describe an adaptation of Gaussian models for offshore conditions. This Offshore and Coastal Dispersion model (OCD) does, however, only incorporate the effect of altered heat fluxes. We have, so far, not not found any references that explicitly take into account the changed dynamics of the wind due to waves. Although we expect the dispersion patterns to be broadly similar to those over mild topography, there is clear evidence that waves alter both the momentum fluxes (Sullivan et al., 2000, 2008; Yang et al., 2013) as well as scalar (heat, moisture and mass) fluxes (Breivik et al., 2015; Jähne and Haußecker, 1998; Yang and Shen, 2017).

The structure of the remainder of this report is as follows. In chapter 2 the basic theoretical tools to describe dispersion is presented. In chapter 3 operational models are briefly described. The wind wave interaction problem is discussed in chapter 4, whereas different airflow models are described in chapter 5. Some evidence towards altered dispersion patterns due to the presence of waves on localized dispersion is given in chapter 6.

2 Theoretical considerations for contaminant transport

Consider the scalar field $c(\boldsymbol{x}, t)$ for the three spatial directions $\boldsymbol{x} = (x, y, z)$ and time t. The scalar field may represent any quantity such as temperature, humidity, or, as in the current review, the concentration of a contaminant. The field c is transported with the wind $\boldsymbol{u}(\boldsymbol{x}, t) = (u(\boldsymbol{x}, t), v(\boldsymbol{x}, t), w(\boldsymbol{x}, t))$, where u, v, and w are the velocity components in the x-, y-, and z-direction, respectively.

2.1 Average properties

The dispersion of c with the wind is governed by turbulent processes. Therefore, both the scalar c and the velocities $\boldsymbol{u}$ fluctuate in time and space. The equations underlying the transport process are for most practical purposes not possible to solve with sufficient detail and accuracy (Pope, 2000).

Averaging has traditionally been used both as a tool to develop simpler flow and transport models, such as Reynolds averaged Navier–Stokes models (RANS), and as tool to analyze measurements and resolved models, such as the fully resolved direct numerical simulation models (DNS) and the partially resolved large eddy simulation models (LES). In turbulence modeling, it is customary to introduce the so called Reynolds averaging, which entails the decomposition of the fields into a mean and fluctuating part. The averaging operation can in principle be defined as the average over time and any of the spatial dimensions (depending on the geometry of the problem), but it can also be defined as the ensemble average, *i.e.* the average over a sufficiently large number of flow realizations. Equations suitable for LES do not rely on averaging, but instead formally use either a spatial or temporal filter (Sagaut and Lee, 2002). Regardless of this, we may write the turbulent field f as the decomposition into a resolved ("mean" quantity $\overline{f}$) and an unresolved ("turbulent" fluctuation quantity f')

$$f(\boldsymbol{x}, t) = \overline{f}(\boldsymbol{x}, t) + f'(\boldsymbol{x}, t), \quad \text{where} \quad \overline{f'} = 0. \tag{2.1}$$

For boundary layer flows, including the atmospheric flow over slowly varying terrain, it is customary to average in time and over the two horizontal directions. A turbulent field can then be written as the decomposition

$$f(x, y, z, t) = \overline{f}(z) + f'(x, y, z, t), \quad \text{where} \quad \overline{f'} = 0. \tag{2.2}$$

The presence of waves introduce a periodic signal into the flow. To analyze such mixed systems with both turbulence and wavy signals, Hussain and Reynolds (1970) instead introduced a triple decomposition

$$f(x, y, z, t) = \underbrace{\overline{f}(z) + \tilde{f}(\boldsymbol{x}, t)}_{\langle f(\boldsymbol{x}, t)\rangle} + f'(\boldsymbol{x}, t), \quad \text{where} \quad \overline{f'} = 0, \quad \overline{\tilde{f}} = 0, \tag{2.3}$$

where $\tilde{f}$ is the wave correlated field and $\langle\cdot\rangle$ represents a phase average. The wave correlated field is hence given as the difference of the phase average and the standard average

$$\tilde{f} = \langle f\rangle - \overline{f}. \tag{2.4}$$

Hussain and Reynolds (1970) showed that wave-correlated momentum fluxes (or stresses) appear in the averaged equations. Hence, momentum stresses can be written as the sum of turbulent, wave correlated, and viscous stresses. Similarly scalar fluxes can be written as the the sum of turbulent, wave correlated and molecular fluxes. The relevance of this, is that waves create stresses (and fluxes) that alter the transport processes.

Even though the description of the flow field can benefit from averaging over homogeneous spatial directions, this does not apply to dispersion modeling because of the localized nature of the source term that leads to a three-dimensional concentration field.

2.2 Eulerian transport equation

The evolution of the scalar field is, in general, governed by an advection-diffusion equation that takes into account both transport by the wind (advection) and molecular mixing processes (diffusion):

$$\partial_t c + \boldsymbol{u} \cdot \nabla c = \nabla(D \nabla c) + S(\boldsymbol{x}, t), \tag{2.5}$$

where $\boldsymbol{u} = (u, v, w)$ is the three dimensional velocity field and D is a, possibly non-constant, diffusivity coefficient, and S is a source term. The left hand side of the equation denotes material transport of the concentration, which is balanced diffusion and source terms on the right hand side. In general, the fields in equation (2.5) are turbulent and must, for most practical purposes, be decomposed in mean and fluctuating parts.

$$\partial_t \langle c \rangle + \langle \boldsymbol{u} \rangle \cdot \nabla \langle c \rangle = \nabla(D \nabla \langle c \rangle - \langle \boldsymbol{u}' c' \rangle) \underset{\text{atm. dispersion}}{\approx} -\nabla \langle \boldsymbol{u}' c' \rangle \,, \tag{2.6}$$

where turbulent stresses $\langle \boldsymbol{u}' c' \rangle$ appear, and in practice replace the molecular diffusion which is negligible for the scales relevant for turbulent dispersion. The turbulent stresses must be modeled, and the most common model assumption is to use an eddy-viscosity hypothesis (similar to Ficks' law) $\langle \boldsymbol{u}' c' \rangle = -D_T \nabla \langle c \rangle$, introducing the isotropic turbulent diffusion parameter D_T, which is non-constant.

Simplifying to a model case with a constant background wind $\langle \boldsymbol{u} \rangle$, a constant point source S, and an isotropic and constant turbulent diffusion parameter D_T, equation (2.6) can be shown to yield the classical Gaussian dispersion models (Stockie, 2011). In the Gaussian framework, the turbulent diffusion parameter is usually modeled as a slightly increasing function of the downwind distance to match experimental data (Hanna et al., 1982).

If, additionally, one assumes that the source term is localized in time, one may derive the so called Gaussian puff models (Stockie, 2011). Furthermore, time varying solutions can be found by integrating Gaussian puffs in time.

If there is significant spatial variation in the wind field, as is the case for flows in complex terrain and/or in the presence of buildings, equation (2.6), Gaussian models are not expected to yield reliable results. Therefore, for such cases the advection diffusion equation must be explicitly solved together with the flow field. This will usually require use of either CFD methodology, using RANS/URANS or LES, on small to medium scales or numerical weather prediction models on larger scales. For all of these cases, except LES, the macroscopic effect turbulent stresses $\langle \boldsymbol{u}' c' \rangle$ must be modeled.

2.3 Lagrangian transport equation

Contaminant transport phenomena may also be studied form a particle point of view. The particles can either be passive fluid parcels that represent gaseous contaminants or physical particles, either in the form of liquid droplets or solid particles, in the case of particular contaminants. Particles suspended in fluids are subject to a range of phenomena (c.f. Schwarzkopf et al., 2012), but for dispersion applications the most important are aerodynamic drag and gravitational pull. If $\boldsymbol{x}_t^p$ and $\boldsymbol{v}^p$ are the position and velocity components of the particle, we have

$$\frac{\mathrm{d}\boldsymbol{x}^p}{\mathrm{d}t} = \boldsymbol{v}^p \tag{2.7}$$

$$\frac{\mathrm{d}\boldsymbol{v}^p}{\mathrm{d}t} = \boldsymbol{F}(\boldsymbol{u} - \boldsymbol{v}^p, \rho, \mu, \rho_p, d_p), \tag{2.8}$$

where $\boldsymbol{F}$ are the forces acting on the particle with density ρ_p and diameter d_p, surrounded by air with density ρ, viscosity μ, and turbulent velocity $\boldsymbol{u}$. Small particles passively follow the air flow, and can be well described by the first equation only with $\boldsymbol{v}^p = \boldsymbol{u}$. On the other hand, larger particles are able to depart from flow streamlines due to increased inertia and gravitational pull.

The air velocity $\boldsymbol{u}$ in equation (2.7) is turbulent, and can be decomposed into a mean ($\langle \boldsymbol{u} \rangle$) and a fluctuating part ($\boldsymbol{u}'$) as discussed above. The effect of the velocity fluctuations on particle trajectories generally needs to be modeled. The exception to this is when the velocity field is sufficiently resolved to capture turbulence, as is the case for DNS or well resolved LES. Models to describe the effect of turbulence falls into three categories, i) the least expensive class of discrete random walk (DRW) models, ii) the more computationally demanding continuous random walk models (CRW), and iii) advanced models based on stochastic differential equation representation of turbulence (SDE) (MacInnes and Bracco, 1992). As noted by Taylor (1922) the role of turbulence is primarily to provide diffusion of particles, *i.e.* to provide departure from mean streamlines. For simple molecular diffusion it can be easily be shown random movement gives identical results to the diffusion equation. However, the diffusive nature of turbulence is much more complex than that of molecular diffusion. To this end one needs to capture history effects, anisotropy and inhomogeneity (Bocksell and Loth, 2001).

2.4 Flow field equations

The flow of fluids on atmospheric scales (ranging from meters up to the scale of the Earth's diameter) is described by the Navier-Stokes equations (Kundu et al., 2012). These equations comprise a coupled set of equations for conservation of mass, momentum and internal (or total) energy. In addition, a thermodynamic equation of state is needed to relate pressure, density and internal energy. For atmospheric conditions, the large range of scales causes variations in the density of the air as a result of hydrostatic pressure differences. As a consequence, the equations must be solved in their compressible form despite the relatively low wind velocities. On medium to large scales, the Earth's rotation must also be taken into account leading to apparent forces known as Coriolis forces. The Navier–Stokes equations can be supplemented by tracer equations to describe transport of species, such as the dispersion of aerosols. See, e.g. Skamarock et al. (2019); IFS47R3III; Bénard

et al. (2010) for examples of the governing equations implemented in various operational numerical weather prediction models.

One form of the Navier–Stokes equations commonly used in atmospheric flows, and which is applicable for local dispersion problems, is the Boussinesq approximation (c.f Kundu et al., 2012). In this approximation, density is assumed to be slowly varying compared to velocities and to depend on temperature only, $\rho = \rho_0 + \rho'(T)$, where ρ_0 is a reference density and T is the temperature. The constraint of a temperature dependent density is only valid on small vertical scales, *i.e.* heights less than 10 km.

The equations for mass conservation and momentum, using the mean $\langle\cdot\rangle$ to signify either averaging suitable for RANS equations or filtering suitable for LES equations, are

$$\nabla \cdot \langle \boldsymbol{u} \rangle = 0 \tag{2.9}$$

$$\frac{\mathrm{D}\langle \boldsymbol{u} \rangle}{\mathrm{D}t} + 2\boldsymbol{\Omega} \times \langle \boldsymbol{u} \rangle = -\frac{1}{\rho_0}\nabla \langle p' \rangle + \nabla \cdot \langle \boldsymbol{\tau} \rangle + \frac{\langle \rho' \rangle}{\rho_0} g, \tag{2.10}$$

where $\boldsymbol{u} = (u, v, w)$ is the three dimensional velocity field, p' is the pressure perturbation about the hydrostatic pressure (found by integration of $\mathrm{d}p_0/\mathrm{d}z = -\rho_0 g$), g is the gravitational acceleration, ρ' is the density perturbation from the base density ρ_0. The rotation of the Earth is included in the Coriolis term, where $\boldsymbol{\Omega}$ denote the rotation vector of earth. Furthermore, momentum stresses denoted $\boldsymbol{\tau}$, may contain unresolved turbulent stresses as well as viscous stresses. Note that, on larger scales, viscous stresses are often neglected and replaced by a drag model. In terms of the Boussinesq approximation, the air density can be written as $\rho = \rho_0[1 + \alpha(T - T_0)]$, where $\rho_0(T_0)$ and T_0 are reference values, and where α is the thermal expansion coefficient. To complete the set of equations, a transport equation for temperature is needed. The temperature equation can be derived from thermodynamic relations, either in the form of the actual temperature or the potential temperature. The latter form is preferred in literature. See McWilliams (2006); Kundu et al. (2012) for derivations and different forms of the energy equation.

3 Operational contaminant transport

3.1 Plumes, puffs and atmospheric stability

The solution to the advection diffusion equation 2.5 can be written as translation of Gaussian distribution functions as described above. This leads to Gaussian dispersion models (Stockie, 2011). The parameters employed in this model are determined by the roughness of the terrain and by meteorological conditions, such as the strength of the wind and the balance of influx and outflux of radiation. The meteorological conditions are often classified on a five-graded scale of atmospheric stability, known as the Pasquill-Gifford-Turner stability classes (Pasquill, 1961), ranging from class A (very unstable) to class F (very stable). Stability class D is denoted neutral stability. An exhaustive description of Gaussian models can be found in Hanna et al. (1982), but the topic received considerable attention during several decades, and informative references include Batchelor (1950); Hanna et al. (1977); Pasquill and Smith (1983); Turner (1994). Gaussian models may handle both continuous and instantaneous releases. For continuous releases, the duration of the release is typically much longer than the time required for the contaminant to reach the location of interest. In this case, the results will only depend on position relative to the release point. For releases with short release duration compared to the transport time, the results and model parameters will also typically depend on time. These models are often denoted *Gaussian puff models*. Provided that the underlying model assumptions are properly taken into account, Gaussian models may provide good estimates for distance ranging from a few hundred meters up to approx. 10 km. Hanna et al. (1985) describe an adaptation of Gaussian models to account for offshore conditions, based on an assumption that the main differences between offshore and onshore dispersion is the altered mixing height, see e.g (Stull, 1988; Sempreviva and Gryning, 2000), and stability conditions. Based on these assumptions, the authors discuss formulas to tune the parameters of the Gaussian models. Note, however, that the effect of waves are not taken into account.

Below, some selected models will be briefly described, and discussed with a view to dispersion over sea.

3.2 Aloha, the NOAA dispersion model

Aloha® (Jones et al., 2013), developed by the National Oceanic and Atmospheric Administration (NOAA) is a dispersion tool for airborne chemicals with emphasis on source modeling. The air dispersion is handled by a Gaussian model in which the dispersion parameters (to determine the width of the plume) can either be inserted automatically from wind measurements or manually by an estimate of the local wind at 10 m and an assessment of the atmospheric stability according to the Pasquill-Gifford-Turner classes. If wind measurements are available, the stability class can be determined by the standard deviation of wind direction (Pasquill, 1979). Otherwise, the recommendations are as follows: In daytime, the stability class is determined based on an estimate of solar insolation (strong, moderate, slight) whereas in the nighttime the stability is based on cloud cover estimation (< 50%,> 50%). If wind measurements are available, the stability class is set according to the standard deviation of wind direction. This is in line with the recommendation of

Pasquill (1979). Note that, for dispersion over water, Jones et al. (2013) recommends using stable conditions regardless of solar insolation and cloud cover, which is in line with Hanna et al. (1985).

3.3 ARGOS

ARGOS[1] is a well known crisis management tool based on the RIMPUFF dispersion model. RIMPUFF (Thykier-Nielsen et al., 1999) was originally developed to be valid for short distances up to 30 km, but according to the documentation is can now be used for dispersion up to several hundreds of kilometers from the source. In order to capture larger variations in the wind field than standard Gaussian models, RIMPUFF uses a book-keeping algorithm to model a continuous release as a series of individual puffs that are advected, diffused and deposited according to the local meteorology. The model may use meteorological data either from a numerical weather prediction model or from measurements and the parameters are determined in the same manner as in Aloha®. Marine boundary layer effects enter only through the wind field provided either by measurements or meteorological models.

3.4 SNAP, a particle based dispersion model

The meteorological office of Norway (met.no), has developed the Severe Nuclear Accident Program (SNAP) (Saltbones et al., 1996, 1998; Bartnicki et al., 2011). The model uses wind data from numerical weather prediction models and a Lagrangian particle model to describe dispersion. A random walk model is used to represent the effects of turbulence, and marine atmospheric boundary layer effects enter the model only through wind field from the numerical weather prediction model. The model has been used to simulate the dispersion of radioactive particles from the Chernobyl accident and of volcanic ash from the 2010 eruption at Eyjafjallajökull in Iceland.

[1] https://pdc-argos.com

4 Wind wave interaction

4.1 The marine atmospheric boundary layer

The interaction of waves and wind occur in the marine atmospheric boundary layer (MABL) which in many ways is similar to the atmospheric boundary layer over land (ABL), see figure 4.1 for an illustration. The atmospheric boundary layer denotes the lowermost part of the atmosphere where the presence of the ground modifies the wind field. In the ABL the horizontal transport of momentum and scalars is dominated by the transport with the mean wind, and the vertical transport is dominated by turbulence. Turbulence can be produced by shear caused by the velocity differences between the top of the ABL and the ground, as well as by the interaction of the mean wind with terrain, vegetation or buildings. Temperature differences between the ground and the air may also influence the turbulence, with the intensity of turbulence increasing over warmer ground and decreasing over colder ground.

The dynamics of the ABL is usually described in a one-dimensional framework (Stull, 1988), and all meteorological models represent the influence of the ground by a one-dimensional drag law (see section 5.1). For the flow over water waves, such drag laws are believed to be suitable for short and slow waves, where the momentum transfer is from the air to the sea. In the case of long and fast waves, where the momentum transfer is reversed (Sullivan et al., 2008; Sullivan and McWilliams, 2010), these drag laws are not expected to be valid.

4.2 Water waves

The flow of air and the flow of water are coupled at the water surface, as shown schematically in figure 4.1, across which velocities vary continuously while the jump in stresses is balanced by surface tension (see e.g. Lamb, 1924). Whenever the surface is brought out of equilibrium, gravity or surface tension act to restore equilibrium, thus leading to wave motion. The evolution of the surface $\eta(x, y, t)$ can to first order be described by a so called inviscid approximation

$$\frac{\mathrm{d}\eta}{\mathrm{d}t} + u\frac{\mathrm{d}\eta}{\mathrm{d}x} + v\frac{\mathrm{d}\eta}{\mathrm{d}y} = w, \quad \nabla^2\phi = 0, \quad \text{where} \quad (u, v, w) = \nabla\phi, \tag{4.1}$$

where x and y are the horizontal directions, u and v are the horizontal water velocities and w is the vertical velocity. The implication of the inviscid assumption is that velocities are irrotational and given by a velocity potential ϕ. To solve the above equations one needs to apply boundary conditions. Note that the surface η is part of the boundary, thus complicating the solution.

In its simplest form, the solution to this set of equations give rise to the so called Airy solution for a monochromatic propagating wave

$$\eta(x, y, t) = a\sin(\boldsymbol{k}\cdot\boldsymbol{x}_h - ct), \tag{4.2}$$

where a is the amplitude of the wave, $k = 2\pi/\lambda$ is the magnitude of the wave number number vector $\boldsymbol{k} = (k_x, k_y)$, and $\boldsymbol{x}_h = (x, y)$ denotes the horizontal directions. The water velocities caused by

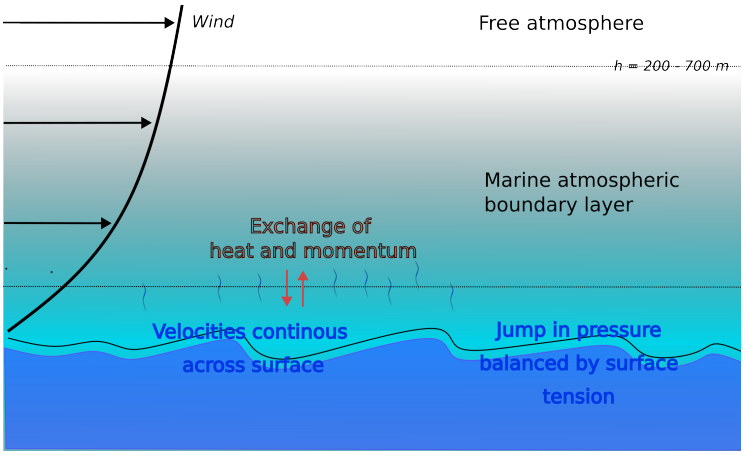

Figure 4.1 The marine atmospheric boundary layer.

the wave are described by $\phi(x, y, z, t) = ak \exp(-kz) \sin(\boldsymbol{k} \cdot \boldsymbol{x} - ct)$. If viscosity is included, the description of the system is much more complicated. This form is not covered in the present review, but is well described in Harrison (1908); Lamb (1924). When the waves become steep, *i.e.* when the quantity ak becomes large, nonlinear effects lead to interaction between different waves (Newman, 2018). Deterministic evolution of non-linearly interacting waves can be obtained by the high order spectral method (HOS) (Dommermuth and Yue, 1987; West et al., 1987). An open source library known as HOS-ocean is described in Ducrozet et al. (2016)[2]. HOS models are suitable to couple with CFD models for air flow calculations (Deskos et al., 2021).

Operational wave models such as WAM, see e.g. (Janssen, 2004; IFS47R3VII), use a transport equation for the discrete frequency spectrum of wave groups as they are unable to explicitly account for all wavenumbers. Using concepts from analytical mechanics, such as Hamiltonians and Lagrangians, and an assumption of slowly varying phase leads to the frequency spectrum transport equation

$$\frac{\mathrm{d}F}{\mathrm{d}t} + \nabla \cdot (\boldsymbol{v}_g F) = S_{\text{wind}} + S_{\text{diss}} + S_{\text{bottom}} + S_{\text{non-linear}}, \tag{4.3}$$

where $\boldsymbol{v}_g$ is the group velocity, $F = F(f, \theta, x, y, t)$ is the spectral density for waves with frequency $f = \omega/2\pi$ and direction of propagation $\theta = \text{atan}(k_y/k_x)$. The source terms are forcing due to wind S_{wind}, dissipation due to white capping S_{diss}, bottom friction S_{bottom} and non-linear wave-wave interactions $S_{\text{non-linear}}$. The wind input in the WAM is adapted from the Miles mechanism (Janssen, 1991).

4.3 Wave growth

The mechanism responsible for creating waves relies on the phase shift of the aerodynamic pressure relative to the wave shape (Miles, 1957). According to Miles (1957) the evolution of the wave amplitude can be written as

$$a(t) = a_0 \exp(\omega\zeta t/2), \quad \zeta = \frac{\rho_a}{\rho_w}\beta, \quad \omega = cak, \tag{4.4}$$

[2]The corresponding code can be found at GitHub: `https://github.com/LHEEA/HOS-ocean`

where the Miles growth rate, β, can be represented in terms of surface pressure misalignment (form drag) and viscous stresses (Belcher and Hunt, 1998; Meirink and Makin, 2000). Although the formula is simple, the functional dependence of the growth rate parameter on environmental parameters such as wind speed, wave height, wave steepness and wind wave alignment is still an unresolved problem (Sullivan and McWilliams, 2010).

Miles (1957, 1959a,b, 1962) attributed this phase shift to the critical-layer instability mechanism. The critical-layer occurs at the center of the Kelvin cats-eyes which are recirculating regions, created by wave induced motion, some distance from the surface. The existence of the critical layer has been confirmed numerically (Sullivan et al., 2000; Kihara et al., 2007), in the laboratory Buckley and Veron (2016), and in the field Hristov et al. (2003). Recently, Carpenter et al. (2022) also presented strong evidence of the relevance of the critical-layer mechanism based on laboratory experiments and stability analysis.

Miles assumed quasi-laminar flow in which turbulent effects only contribute to maintaining the mean flow and do not influence the wave-induced flow. Turbulence will, however, also contribute to the wave-induced flow. This was demonstrated by Belcher and Hunt (1993, 1998) who, based on the non-separated sheltering idea introduced by Jeffreys (1925), postulated that the wave correlated turbulent stresses are important to establish the phase shift of the pressure that drive the wave growth. This conjecture was supported by the detailed numerical study of Åkervik and Vartdal (2019), where turbulence was shown to be important for slow waves, but not for fast waves.

4.4 Wind-wave spectrum: Wind sea and swell sea

The wind excites a range of wave lengths, leading to a broadband spectrum in which wavelengths with phase speeds comparable to the local wind appear to dominate. This is reflected in the Pierson Moskovits equilibrium spectrum (Pierson Jr and Moskowitz, 1964). The wave age is defined by the ratio between the phase speed of the waves and the wind, and equilibrium occurs roughly at the wave age $c/U_{10} \approx 1.2$. According to the JONSWAP spectrum (Hasselmann et al., 1973), equilibrium seas are newer obtained because growing waves interact non-linearly to form new wave components (Zakharov, 1968; Janssen, 2004).

Wind waves, or young waves, propagate mainly in the local wind direction with a relatively low wave speed $c < 1.2U_{10}$. Faster waves are known as swell waves or old waves. Swell waves with long wavelengths can propagate the oceans with little damping, and their propagation direction need not be aligned with the local wind after some distances (Sullivan et al., 2008). Observed wave spectra may contain both wind sea waves and swells at the same time (Semedo et al., 2015), and simple one peak parameterizations, such as the Pierson-Moskowits and the JONSWAP spectra, are not expected to give a good representation of the waves. Several two-peak spectra exist, see e.g. Ochi and Hubble (1976); Soares (1984); Torsethaugen (1993), which may provide better representation of the sea states.

4.5 Classification of waves

A mixed sea state of wind waves and swell waves can have the same period and wave height as a young sea without swell (Semedo et al., 2011), and it can be difficult to classify the type of waves

present in a measured wave spectrum. A better classification can be obtained by also evaluating the mean wave direction (Semedo et al., 2015).

Boukhanovsky et al. (2007) incorporated the wave direction to arrive at a classification scheme, and used the wave steepness at the peak frequency to determine whether the sea state is swell or wind dominated. Applying their method to a 10 year hindcast of the North Sea, they found that pure wind waves were the dominant sea state (60-65 %), with mixed sea states of "fresh" swells and wind sea were the second most dominant sea state (13-23 %). The authors claim that their method can be applied to any region in the world, in contrast to the Torsethaugen spectrum (Torsethaugen, 1993) which appear to best describe the Norwegian sea.

Better classification of sea states can be obtained by using simultaneous information on the wind and the waves. Semedo et al. (2011) analyses wave data from the 45 year European Centre for Medium-Range Weather Forecasts (ECMWF) Re-Analysis (ERA-40). Based on concurrent wind data from the meteorological model and the wave spectrum from the coupled wave model, they used the standard WAM (IFS47R3VII) criterion to discriminate the two sea states and found that the global oceans are strongly dominated by swell waves. To properly account for local winds along coastline and the influence of local geometry and bathymetry on the waves, Semedo et al. (2015) used the nested NORA10 (Reistad et al., 2011) data set to focus on the the Nordic seas (North sea, Norwegian sea and the Barents sea). In line with Boukhanovsky et al. (2007), they find that the North Sea is wind sea dominated. On the other hand, the Norwegian seas are clearly swell dominated, with swells carrying more than 65 % of the wave energy in the winter and 85-90 % in the summer.

The prevalence of swell waves in the Norwegian sea may impact the dispersion characteristics of released contaminants, as there is evidence that swell waves lead to an effective transport away from the surface (Li et al., 2019; Åkervik, 2022) through a vertical pumping mechanism. Contrast this to the case of wind waves, in which there is evidence of a net vertical transport towards the surface. We will discuss the balance of these two conflicting mechanisms further in sections 6.2 and 6.3 below.

5 Airflow models

5.1 Meteorological wave averaged airflow models

In the Nordic countries, short term operational forecasts are provided by a convective-scale weather prediction model that is operated by a cooperative effort between the Finnish Meteorological Institute (FMI), MET Norway and Swedish Meteorological and Hydrological Institute (SMHI) through the *MetCoOp* collaboration (Müller et al., 2017). The core of the model is based on the AROME model developed by Météo-France (Seity et al., 2011), which again is based on the HARMONIE model from the HIRLAM consortium[3]. The AROME-MetCoOp model is forced, at the lateral and upper boundaries by, the global ensemble forecasts provided by the European Centre for Medium-Range Weather Forecast's Integrated Forecast System (described in the report series IFS47R3I; IFS47R3II; IFS47R3III; IFS47R3IV; IFS47R3V; IFS47R3VI; IFS47R3VII).

Whichever numerical weather prediction model (such as ECMWF or AROME) that is used, the effect of surface waves is modeled by a surface scheme using a drag formulation (IFS47R3IV; Le Moigne et al., 2018). Surface fluxes that relate the surface conditions to the flow are typically formulated as

$$\tau_{tot} = \rho C_D |U_n|^2, \tag{5.1}$$

where $|U_n|$ is the velocity magnitude and C_D is the drag coefficient given by Monin-Obukhov theory (Foken, 2006). Thus we have $C_D = \text{fcn}(z_0, \mathcal{L})$, where z_0 is a roughness length and $\mathcal{L}$ is the Obukhov length describing the degree of stratification. At the interface between the surface and the atmosphere, each grid-box is divided into fractions (tiles) that characterizes the type of surface the airflow is subject to. For onshore conditions the roughness length varies from less than a centimeter for ice caps and glaciers, through some decimeters for grasslands, to more than one meter for forested areas (IFS47R3IV). Whereas the roughness length for onshore conditions are related to the geometric shape of the roughness elements, this does not apply to offshore conditions (Hasse, 1986). Charnock (1955) used dimensional analysis to obtain a relation between the sea state and the roughness length

$$z_0 = \alpha_{Ch} u_*^2 / g, \tag{5.2}$$

where u_* is the friction velocity and g is the gravitational acceleration. Charnock proposed that the parameter $\alpha_{Ch} \approx 0.0067$ is a constant. According to Deskos et al. (2021), however, this parameter depends on several quantities, such as sea state and wind speed, and is reported to be in the range $0.0144 \leq \alpha_{Ch} \leq 0.0354$.

It is important to note that meteorological models only use a one-dimensional description of the waves, and thus only handles the influence of waves through a bulk transfer coefficient averaged over the waves.

[3]HIRLAM (High Resolution Limited Area Model) is a research cooperation of 11 European meteorological institutes (http://www.hirlam.org).

5.2 High fidelity simulations on laboratory scales

Early work on high-fidelity wave-phase resolved numerical modeling of the flow over waves used Reynolds averaged Navier-Stokes (RANS) models for monochromatic waves (Gent and Taylor, 1976; Van Duin and Janssen, 1992). These studies showed that the computed results are sensitive to the choice of turbulence closure scheme (Van Duin and Janssen, 1992), and suitable closures were proposed (Mastenbroek et al., 1996; Li et al., 2000; Meirink and Makin, 2000).

Increased computational capabilities led to studies using direct numerical simulation (DNS) (Sullivan et al., 2000; Kihara et al., 2007; Yang and Shen, 2009, 2010). These, and others, have provided insight into the wave correlated motion (Sullivan et al., 2000), the structure of the turbulence (Yang and Shen, 2009, 2010), and the low Reynolds number understanding of the Miles mechanism versus the non-separated sheltering (Kihara et al., 2007). Due to the strict resolution requirements inherent to DNS, only low Reynolds numbers have been considered so far. This also applies to studies devoted to wall resolved large eddy simulation (LES) (Åkervik and Vartdal, 2019). Meirink and Makin (2000) used the results from simulations with low Reynolds number RANS models to discuss the Reynolds number effects on the drag. They found reasonable agreement with Sullivan et al. (2000) at low Reynolds number, but also showed that there are significant differences between the form drag obtained at low and intermediate Reynolds numbers.

Note that the extreme computational cost associated with such high fidelity models implies that they can only be used to gain insight into the physics of the wind-wave interaction problem, and are not suitable for operational conditions.

5.3 Wall-modeled wave-phase resolved LES: Towards high fidelity simulations on operational scales

Wall-modeled large eddy simulation (LES) can bridge the gap between small and large scales, and can therefore capture the action of the waves on the wind, at scales that are meaningful for local dispersion, without the computational cost of DNS and wall-resolved LES.

In a traditional, or wall-resolved, LES it is necessary to resolve the near-surface eddies which becomes smaller with increasing Reynolds number, requiring ever more computational resources. In a wall-modeled LES, the resolution requirements are relaxed because the effect of the near-surface eddies are modeled (Bose and Park, 2018), removing the Reynolds number scaling. An important difference between wall-modeled LES modeling of for the flow offshore and onshore relates to the definition of the aerodynamic drag, represented by a roughness parameter. For the flow in onshore atmospheric flows, the roughness length depend mainly on the geometrical feature of the obstacles. The drag resulting from the action of waves is, however, a much more complicated process that depends on the dynamic behavior of the waves (Hasse, 1986). Yang et al. (2013) discuss several different wall models applied to the flow over waves, and show that a combined wave-kinematics model provide the most reliable results.

Sullivan et al. (2008) use wall-modeled LES to study the flow over swell waves, both in terms of waves propagating in the same direction as the wind and waves opposing the wind. They resolve

100 m long swell waves on a large computational domain, and use a constant roughness length of 2×10^{-4} m to mimic the action of short waves riding on top of the long waves. The computed results agree well with the data of the CBLAST campaign (Edson et al., 2004). For swells that propagate in the direction of the wind, the LES data show a near collapse of turbulence in the planetary boundary layer caused by a combination of the thrusting action of swells aligned with the mean wind, and the creation of a low level jet at a height of about 20 % of the wavelength. Conversely, swells that oppose the wind increase turbulence levels over the depth of the boundary layer, and the drag increase fourfold compared to a flat boundary layer flow. A major finding of this study is that the action of swell waves on the wind is not limited to a region close to the surface, but instead alters the wind throughout the boundary layer. In a follow-up paper, Sullivan et al. (2014) use a prescribed time evolving spectrum instead of a simple moving wave. For non-equilibrium waves, *i.e.* either fast swells or slow wind waves, they find that the wind profiles can deviate significantly from the Monin-Obukhov theory, which forms the backbone of meteorological models. Hara and Sullivan (2015) develop analysis tools, mainly in the form of momentum and energy budgets, suitable to analyze the wavy flow. For low wave age, *i.e.* high wind speed compared to wave propagation speed, they show that enhanced wave induced stresses results in a reduced turbulent stress, and less wind shear, causing the roughness length to increase.

While Sullivan et al. (2008); Hara and Sullivan (2015) consider only prescribed wave motion, Yang et al. (2013) couple a LES solver with the High-order Spectral Method (abbreviated as HOS, see section 4.2) to compute the evolution of the air flow and the wave motion simultaneously. Yang et al. (2013) and Liu et al. (2010) simulate the evolution of both monochromatic and broadband spectrum waves. Simulating a spectrum of waves, they find that the growth of long waves agrees well with simple monochromatic waves, whereas the growth of short waves do not. Shorter waves appear to be sheltered from the action of the wind when they ride on top of longer waves. Consequently, the full spectrum needs to be considered for the evolution of short waves, whereas longer waves can be described as single waves.

These studies show that methods are now available that accurately describe the altered dynamics of the marine atmospheric boundary layer caused by the effect of waves.

5.4 Simplified wave-phase resolved models

Wave-phase resolved simplified models seek to separate different aspects of the flow such as shear generated turbulence, wave generated turbulence, wave geometry, and wave kinematics.

Åkervik and Vartdal (2019) studied the flow over monochromatic linear waves at different Reynolds numbers and wave numbers using wall-resolved LES. The computational results show that, with increasing wave age, the turbulent and wave-induced stresses separate in the vertical direction, so that the wave-induced stresses and turbulent stresses appear to decouple. By decomposing the flow into a wave-kinematics flow and a shear driven flow, they formulated a simplified RANS description. The computational results in combination with this model, show that the wave induced stresses do indeed appear to be dominated by the wave kinematics and decoupled from turbulent stresses for swell waves. Based on this analysis, they developed a simple formula for the form drag as a function of the wave age and Reynolds number. They also show that, for low wave ages, the turbulent stresses

are crucial in determining the wave induced flow field, supporting the well known non-separated sheltering mechanism of Belcher and Hunt (1993, 1998).

Cao et al. (2020); Cao and Shen (2021); Cao et al. (2023) build on Åkervik and Vartdal (2019) to develop a framework for studying the flow over waves, and use data from wall-resolved LES at intermediate Reynolds numbers to validate their framework. While Åkervik and Vartdal (2019) view the total flow as a perturbation about the wave induced flow, Cao and co-workers use the traditional view with the waves as a perturbation about the mean flow (Miles, 1957). Cao and Shen (2021) confirm the findings of Åkervik and Vartdal (2019), that turbulence and wave induced motion decouple for swell waves.

In all the works discussed above (Åkervik and Vartdal, 2019; Cao et al., 2020; Cao and Shen, 2021; Cao et al., 2023), the description of the flow field depends on knowledge of the turbulent stresses obtained from accurate computations using wall-resolved LES. In their current state, they are therefore not suitable as operational models. Further studies are needed to explore if simpler turbulence models can be used to describe the flow at high Reynolds numbers, using data from wall-resolved LES on small scales and wall-modeled LES on large scales as reference. Furthermore, care should be taken in the interpretation of the apparent decoupling of turbulent stresses and wave induced motions for swell waves. Recall the wall-modeled LES study of Sullivan et al. (2008) shows the formation of a low level jet and the corresponding collapse of turbulence in the outer part of the flow.

A simplified model for the flow over waves was developed by Kudryavtsev et al. (2001) and applied to swell waves in Kudryavtsev and Makin (2004). This simplified model, following Belcher and Hunt (1993, 1998), divide the flow in a near-surface region and an outer region. Their model results were compared to experimental data, and confirm the existence of low level jets. It is, however, unclear how turbulence is affected. The model of Kudryavtsev et al. (2001) was developed before the advent of high fidelity LES for the flow over waves, and it would be interesting to use the more complete data sets provided during the last 20 years to reassess their findings.

6 Evidence of altered dispersion characteristic for flow over waves

There appears to be only a handful mechanistic (*i.e.* wave-phase resolved) studies on the transport of scalars in the presence of waves. In this section, we present conclusions from four studies that used wave-phase resolved CFD to quantify transport of scalars above waves.

6.1 Non-localized scalar transport on a laboratory scale

We first consider results from two studies of flow over monochromatic waves at low Reynolds numbers. These studies do not directly relate to dispersion from a localized source, but is relevant to assess heat and mass fluxes.

Sullivan and McWilliams (2002) used direct numerical simulation to study the interaction of simple propagating waves and background stratification. They found that the stratification altered the vertical profiles of both the flow field and the temperature and therefore altered the surface form stress, compared to a neutral background. They also found that the ratio of phase speed to friction velocity (wave age) remained the critical parameter in describing the interaction of wind and waves.

Yang and Shen (2017) studied the transport of passive scalars above waves using direct numerical simulation. They found that the wave-phase-correlated variation of the scalar field strongly depend on the wave age. Interestingly, the mean vertical profiles of the scalar over waves had similar structures as in the turbulent flow over a flat wall. The profiles of the vertical scalar flux in the viscous sublayer do however deviate from the scaling law for flat-wall turbulence, caused by a negative vertical flux region above the windward face of the wave crest.

6.2 Localized source on a laboratory scale

Åkervik (2022) used wall resolved large eddy simulation to study the scalar transport, from a localized source, over monochromatic waves at two different wave ages and over a flat surface. The interaction of the waves and the airflow was described by a volume of fluid method Hirt and Nichols (1981), that enabled transport across the interface. A localized source, consisting of non-interacting Lagrangian particles of different sizes was introduced into a turbulent flow with a similar Reynolds number as in Yang and Shen (2017). For young (slow) waves, there was clear evidence of increased downward transport, as long as the particles had sufficient inertia to depart from the orbital motion of the circulating regions above the waves. On the other hand, for old (fast) waves the wave induced motion caused a net upward motion of the particles leading to higher concentrations downstream. Note that the results from Åkervik (2022), although convincing, were obtained at small spatial scales with a limited span of admissible particle sizes. Similar studies should therefore be performed at larger, atmospheric scales with waves of length 1-100 m, possibly by the use of wall-modeled LES similar to Sullivan et al. (2008).

6.3 Localized source on an operational scale

Li et al. (2019) used wall-modeled LES to simulate the transport of buoyant oil droplet aerosols in wind over monochromatic waves. They considered two cases; one with a flat surface, and one with a long (100 m) propagating swell wave in the same direction as the wind. In both cases a surface roughness was applied at the surface to mimic the effect of short waves. In other words, the effect of wind waves were phase-averaged, as in meteorological models. Therefore, the authors did not address the possible added downward transport provided by wind waves. However, the effect of the long swell waves was resolved.

For all the aerosol sizes studied in the paper (from 2.5 μm to 100 μm), swell waves leads to enhanced suspension, such that the aerosols were pumped away from the surface by the flow perturbations caused by the waves. For the largest aerosols, where deposition at the surface was likely, the presence of swell waves prevented deposition and lead to higher air concentrations.

7 Concluding remarks

This report has reviewed the state of the art in dispersion modeling for turbulent atmospheric flow over water waves.

The single most important factor that determines the dispersion of aerosols is the wind field. Dispersion models can broadly be distinguished by whether they use detailed or simplified knowledge of the flow field. Gaussian *plume* models assume a constant wind and simple parameterization of the turbulent diffusion. For this reason, Gaussian plume models are only expected to give reasonable results over slowly varying terrain and for short distances. On the other hand, Gaussian *puff* models are readily extended to *time* varying flow fields. For flow over complex geometries, such as large terrain variations and/or buildings, it is usually necessary to use computational fluid dynamics (CFD) to accurately describe the flow. Similarly, for long time dispersion over large distances, mesoscale numerical weather prediction models are needed. When using meteorological models for wind input it is common to either use a Lagrangian particle method or a Gaussian puff model. Note, however, that turbulent dispersion is heavily parameterized in meteorological models so that it may be challenging to obtain a good representation of lateral and vertical plume spread. The influence of the ground conditions on the wind is typically modeled by means of the one-dimensional Monin-Obukhov drag theory, where smooth surface give little drag, and rough surfaces give more drag.

Wind waves are caused by wind blowing over the water surface. Short (and slow) waves are in general aligned with the mean wind, since they are newly created by the local wind. Their action is to exert a drag on the wind while they grow in amplitude. On the other hand, long (and fast) waves are often the result of remote high wind events. These waves may propagate large distances and arrive at locations where they are faster than the local wind. They are generally not aligned with the local mean wind, but if they are, they result in a thrust on the wind and can lead to the formation of low level jets and turbulence collapse. This complex behavior is not well described by the current one-dimensional drag theories.

We have not found any references to operational models that explicitly account for the flow field modifications caused by the presence of waves. Waves have traditionally been believed to only mildly affect the air flow. However, recent studies show that this is not the case, especially for fast waves. Furthermore, there is some evidence in the literature that slow waves may promote deposition of aerosols on the surface, and therefore lead to reduced air concentrations. Conversely, for fast waves there is evidence that upward transport mechanism not present over land causes suspension of aerosols and therefore leads to faster downstream transport and higher concentrations.

More detailed description of the interaction of waves and wind has been provided the last two decades. First in the form of laboratory scale highly accurate turbulence resolving large-eddy and direct-numerical simulations over simple propagating waves. Thereafter in the form of more approximate wall-modeled large eddy simulations on operational scales and complex waves. The latter provide the state of the art within flow models suitable for operational dispersion modeling on short to intermediate time scales. However, these models are, at present, highly specialized tools suitable for specialists only. We, therefore, envision two possible routes to improve dispersion modeling offshore. The first is to use wall-modeled LES to map out the the parameter space to

arrive at vertical transport velocities suitable for a one-dimensional description. The second is to continue development of wave-resolving simplified models which can provide the wave induced flow modification to the classical one-dimensional operational flow models.

References

Åkervik, E. Aerosol transport in idealized wind-wave systems. Tech. Rep. 22/02547, FFI - Norwegian Defence Research Establishment, 2022. URL https://www.ffi.no/en/publications-archive/aerosol-transport-in-idealized-wind-wave-systems.

Åkervik, E. and Vartdal, M. The role of wave kinematics in turbulent flow over waves. *J. Fluid Mech*, 880:890–915, 2019. URL https://doi.org/10.1017/jfm.2019.708.

Bartnicki, J., Haakenstad, H., and Hov, Ø. Operational SNAP model for remote applications from NRPA. Tech. Rep. no. 12/2011, Norwegian Meteorological Institute (met.no), 2011. URL https://www.met.no/publikasjoner/met-report/met-report-2011/_/attachment/download/7405afe8-7d97-49b3-9d85-aef7b8e5d86d:3f7ed544a977dbcc8432dbdf2102305ea2f533dd/MET-report-12-2011.pdf.

Batchelor, G. The application of the similarity theory of turbulence to atmospheric diffusion. *Q. J. R. Meteorol. Soc.*, 76 (328):133–146, 1950. URL https://doi.org/10.1002/qj.49707632804.

Bauer, P., Thorpe, A., and Brunet, G. The quiet revolution of numerical weather prediction. *Nature*, 525 (7567):47–55, 2015. URL https://doi.org/10.1038/nature14956.

Belcher, S. E. and Hunt, J. C. R. Turbulent shear flow over slowly moving waves. *J. Fluid Mech*, 251:109–148, 1993. URL https://doi.org/10.1017/S0022112093003350.

Belcher, S. E. and Hunt, J. C. R. Turbulent flows over hills and waves. *Annu. Rev. Fluid Mech*, 30:507–38, 1998. URL https://doi.org/10.1146/annurev.fluid.30.1.507.

Bénard, P., Vivoda, J., Mašek, J., Smolíková, P., Yessad, K., Smith, C., Brožková, R., and Geleyn, J.-F. Dynamical kernel of the aladin–nh spectral limited-area model: Revised formulation and sensitivity experiments. *Quarterly Journal of the Royal Meteorological Society: A journal of the atmospheric sciences, applied meteorology and physical oceanography*, 136 (646):155–169, 2010. URL https://doi.org/10.1002/qj.522.

Bocksell, T. L. and Loth, E. Random walk models for particle diffusion in free-shear flows. *AIAA journal*, 39 (6):1086–1096, 2001. URL https://doi.org/10.2514/2.1421.

Boris, J., Fulton Jr, J. E., Obenschain, K., Patnaik, G., and Young Jr, T. CT-analyst: Fast and accurate CBR emergency assessment. In *Chemical and Biological Sensing V*, vol. 5416, pp. 1–13 (SPIE, 2004). URL https://doi.org/10.1117/12.542852.

Bose, S. T. and Park, G. I. Wall-modeled large-eddy simulation for complex turbulent flows. *Annu. Rev. Fluid Mech*, 50:535–561, 2018. URL https://doi.org/10.1146/annurev-fluid-122316-045241.

Boukhanovsky, A. V., Lopatoukhin, L. J., and Soares, C. G. Spectral wave climate of the North Sea. *Applied Ocean Research*, 29 (3):146–154, 2007. URL https://doi.org/10.1016/j.apor.2007.08.004.

Breivik, Ø., Mogensen, K., Bidlot, J.-R., Balmaseda, M. A., and Janssen, P. A. Surface wave effects in the NEMO ocean model: Forced and coupled experiments. *Journal of Geophysical Research: Oceans*, 120 (4):2973–2992, 2015. URL https://doi.org/10.1002/2014JC010565.

Britter, R. and Hanna, S. Flow and dispersion in urban areas. *Annu. Rev. Fluid Mech*, 35 (1):469–496, 2003. URL https://doi.org/10.1146/annurev.fluid.35.101101.161147.

Buckley, M. P. and Veron, F. Structure of the airflow above surface waves. *Journal of Physical Oceanography*, 46 (5):1377–1397, 2016. URL https://doi.org/10.1175/JPO-D-15-0135.1.

Cao, T., Deng, B.-Q., and Shen, L. A simulation-based mechanistic study of turbulent wind blowing over opposing water waves. *J. Fluid Mech*, 901:A27, 2020. URL https://doi.org/10.1017/jfm.2020.591.

Cao, T., Liu, X., Xu, X., and Deng, B. Investigation on mechanisms of fast opposing nonlinear water waves influencing overlying wind turbulence using large-eddy simulation and theoretical models. *Phys. Fluids*, 35:015148, 2023. URL https://doi.org/10.1063/5.0132131.

Cao, T. and Shen, L. A numerical and theoretical study of wind over fast-propagating water waves. *J. Fluid Mech*, 919:A38, 2021. URL https://doi.org/10.1017/jfm.2021.416.

Carpenter, J., Buckley, M., and Veron, F. Evidence of the critical layer mechanism in growing wind waves. *Journal of Fluid Mechanics*, 948:A26, 2022. URL https://doi.org/10.1017/jfm.2022.714.

Charnock, H. Wind stress on a water surface. *Quarterly Journal of the Royal Meteorological Society*, 81 (350):639–640, 1955. URL https://doi.org/10.1002/qj.49708135027.

Deskos, G., Lee, J. C., Draxl, C., and Sprague, M. A. Review of wind–wave coupling models for large-eddy simulation of the marine atmospheric boundary layer. *Journal of the Atmospheric Sciences*, 78 (10):3025–3045, 2021. URL https://doi.org/10.1175/JAS-D-21-0003.1.

Dommermuth, D. G. and Yue, D. K. A high-order spectral method for the study of nonlinear gravity waves. *J. Fluid Mech*, 184:267–288, 1987. URL https://doi.org/10.1017/S002211208700288X.

Ducrozet, G., Bonnefoy, F., Le Touzé, D., and Ferrant, P. HOS-ocean: Open-source solver for nonlinear waves in open ocean based on High-Order Spectral method. *Computer Physics Communications*, 203:245–254, 2016. URL https://doi.org/10.1016/j.cpc.2016.02.017.

Edson, J., Crofoot, R., McGillis, W., and Zappa, C. Investigations of flux-profile relationships in the marine atmospheric boundary layer during CBLAST. In *Extended Abstracts, 16th Symp. on Boundary Layers and Turbulence* (2004). URL https://www.researchgate.net/publication/229003543_Investigations_of_flux-profile_relationships_in_the_marine_atmospheric_boundary_layer_during_CBLAST/link/0fcfd51472da9d5eae000000/download.

Foken, T. 50 years of the Monin–Obukhov similarity theory. *Boundary-Layer Meteorology*, 119:431–447, 2006. URL https://doi.org/10.1007/s10546-006-9048-6.

Gent, P. R. and Taylor, P. A. A numerical model of the air flow above water waves. *J. Fluid Mech*, 77 (1):105–128, 1976. URL https://doi.org/10.1017/S0022112076001158.

Hanna, S., Briggs, G., Deardorff, J., Egan, B., Gifford, F., and Pasquill, F. AMS workshop on stability classification schemes and sigma curves—summary of recommendations. *Bulletin of the American Meteorological Society*, pp. 1305–1309, 1977. URL https://www.jstor.org/stable/26218024.

Hanna, S. R., Briggs, G. A., and Hosker Jr, R. P. Handbook on atmospheric diffusion. Tech. rep., National Oceanic and Atmospheric Administration, Oak Ridge, TN USA, 1982. URL https://doi.org/10.2172/5591108.

Hanna, S. R., Schulman, L. L., Paine, R. J., Pleim, J. E., and Baer, M. Development and evaluation of the offshore and coastal dispersion model. *Journal of the Air Pollution Control Association*, 35 (10):1039–1047, 1985. URL https://doi.org/10.1080/00022470.1985.10466003.

Hara, T. and Sullivan, P. P. Wave boundary layer turbulence over surface waves in a strongly forced condition. *J. Fluid Mech*, 45:868–883, 2015. URL https://doi.org/10.1175/JPO-D-14-0116.1.

Harrison, W. J. The influence of viscosity on the oscillations of superposed fluids. *"Proc. Roy. Soc. Lond. Ser. A"*, 2 (1):396–405, 1908. URL https://doi.org/10.1112/plms/s2-6.1.396.

Hasse, L. On Charnock's Relation for the Roughness at Sea. In *Oceanic Whitecaps*, pp. 49–56 (Springer, 1986). URL https://doi.org/10.1007/978-94-009-4668-2_5.

Hasselmann, K., Barnett, T. P., Bouws, E., Carlson, H., Cartwright, D. E., Enke, K., Ewing, J., Gienapp, A., Hasselmann, D., Kruseman, P., et al. Measurements of wind-wave growth and swell decay during the joint north sea wave project (jonswap). *Ergaenzungsheft zur Deutschen Hydrographischen Zeitschrift, Reihe A*, 1973. URL https://hdl.handle.net/21.11116/0000-0007-DD3C-E.

Hirt, C. W. and Nichols, B. D. Volume of fluid (VOF) method for the dynamics of free boundaries. *Journal of computational physics*, 39 (1):201–225, 1981. URL https://doi.org/10.1016/0021-9991(81)90145-5.

Hristov, T. S., Miller, S. D., and Friehe, C. A. Dynamical coupling of wind and ocean waves through wave-induced air flow. *Nature*, 422:55–58, 2003. URL https://doi.org/10.1038/nature01382.

Hussain, A. K. M. F. and Reynolds, W. C. The mechanics of an organized wave in turbulent shear flow. *J. Fluid Mech*, 41:241–258, 1970. URL https://doi.org/10.1017/S0022112070000605.

IFS47R3I. IFS Documentation CY47R3 - Part I: Observations . 2021. URL https://doi.org/10.21957/ycow5yjr1.

IFS47R3II. IFS Documentation CY47R3 - Part II: Data observations. 2021. URL https://doi.org/10.21957/t445u8kna.

IFS47R3III. IFS Documentation CY47R3 - Part III: Dynamics and numerical procedures. 2021. URL https://doi.org/10.21957/b18qsx663.

IFS47R3IV. IFS Documentation CY47R3 - Part IV: Physical processes. 2021. URL https://doi.org/10.21957/eyrpir4vj.

IFS47R3V. IFS Documentation CY47R3 - Part V: Ensemble prediction system. 2021. URL https://doi.org/10.21957/zw5j5zdz5.

IFS47R3VI. IFS Documentation CY47R3 - Part VI: Technical and computational procedures. 2021. URL https://doi.org/10.21957/3oxwrgb0s.

IFS47R3VII. IFS Documentation CY47R3 - Part VII: ECMWF Wave model. 2021. URL https://doi.org/10.21957/zz4bj65vr.

Jähne, B. and Haußecker, H. Air-water gas exchange. *Annu. Rev. Fluid Mech*, 30 (1):443–468, 1998. URL https://doi.org/10.1146/annurev.fluid.30.1.443.

Janssen, P. *The interaction of ocean waves and wind* (Cambridge University Press, 2004). URL https://doi.org/10.1017/CBO9780511525018.

Janssen, P. A. Quasi-linear theory of wind-wave generation applied to wave forecasting. *Journal of physical oceanography*, 21 (11):1631–1642, 1991. URL https://doi.org/10.1175/1520-0485(1991)021<1631:QLTOWW>2.0.CO;2.

Jeffreys, H. On the formation of water waves by wind. *Proc. Lond. Ser. A, Containing Papers of a Mathematical and Physical Character*, 107 (742):189–206, 1925. URL https://doi.org/10.1098/rspa.1925.0015.

Jones, R., Lehr, W., Simecek-Beatty, D., and Reynolds, R. M. ALOHA (Areal Locations of Hazardous Atmospheres) 5.4.4: Technical Documentation. Tech. Rep. NOS OR&R 43, U. S. Dept. of Commerce, Seattle, WA: Emergency Response Division, NOAA, 2013. URL https://response.restoration.noaa.gov/sites/default/files/ALOHA_Tech_Doc.pdf.

Joshi, M. M., Gregory, J. M., Webb, M. J., Sexton, D. M., and Johns, T. C. Mechanisms for the land/sea warming contrast exhibited by simulations of climate change. *Climate dynamics*, 30 (5):455–465, 2008. URL https://doi.org/10.1007/s00382-007-0306-1.

Kihara, N., Mizuya, T., and Ueda, H. Relationship between airflow at the critical height and momentum transfer to the traveling waves. *Phys. Fluids*, 19:015102, 2007. URL https://doi.org/10.1063/1.2409736.

Kudryavtsev, V., Makin, V., and Meirink, J. Simplified model of the air flow above waves. *Boundary-layer meteorology*, 100:63–90, 2001. URL https://doi.org/10.1023/A:1018914113697.

Kudryavtsev, V. N. and Makin, V. K. Impact of swell on the marine atmospheric boundary layer. *Journal of physical oceanography*, 34 (4):934–949, 2004. URL https://doi.org/10.1175/1520-0485(2004)034<0934:IOSOTM>2.0.CO;2.

Kundu, P. K., Cohen, I. M., and Dowling, D. R. *Fluid Mechanics* (Elsevier Academic Press, 2012), 5. ed.

Lamb, H. *Hydrodynamics* (University Press, 1924).

Le Moigne, P., Albergel, C., Boone, A., Belamari, S., Decharme, B., Dumont, M., and Masson, V. SURFEX SCIENTIFIC DOCUMENTATION. 2018. URL http://www.umr-cnrm.fr/surfex/IMG/pdf/surfex_scidoc_v8.1.pdf.

Li, M., Zhao, Z., Pandya, Y., Iungo, G. V., and Yang, D. Large-eddy simulations of oil droplet aerosol transport in the marine atmospheric boundary layer. *Atmosphere*, 10 (8):459, 2019. URL https://doi.org/10.3390/atmos10080459.

Li, P., Xu, D., and Taylor, P. A. Numerical modelling of turbulent airflow over water waves. *Bound. Lay. Met.*, 95 (3):397–425, 2000. URL https://doi.org/10.1023/A:1002677312259.

Liu, Y., Yang, D., Guo, X., and Shen, L. Numerical study of pressure forcing of wind on dynamically evolving water waves. *Phys. Fluids*, 22 (4):041704, 2010. URL https://doi.org/10.1063/1.3414832.

MacInnes, J. and Bracco, F. Stochastic particle dispersion modeling and the tracer-particle limit. *Phys. Fluids*, 4 (12):2809–2824, 1992. URL https://doi.org/10.1063/1.858337.

Mastenbroek, C., Makin, V. K., Garat, M. H., and Giovanangeli, J.-P. Experimental evidence of the rapid distortion of turbulence in the air flow over water waves. *J. Fluid Mech*, 318:273–302, 1996. URL https://doi.org/10.1017/S0022112096007124.

McWilliams, J. C. *Fundamentals of geophysical fluid dynamics* (Cambridge University Press, 2006).

Meirink, J. F. and Makin, V. K. Modelling low-reynolds-number effects in the turbulent air flow over water waves. *J. Fluid Mech*, 415:155–174, 2000. URL https://doi.org/10.1017/S0022112000008624.

Miles, J. W. On The Generation of Surface Waves By Shear Flows. *J. Fluid Mech*, 3:185–204, 1957. URL https://doi.org/10.1017/S0022112057000567.

Miles, J. W. On the generation of surface waves by shear flows. Part 2. *J. Fluid Mech*, 6 (4):568–582, 1959a. URL https://doi.org/10.1017/S0022112059000830.

Miles, J. W. On the generation of surface waves by shear flows Part 3. Kelvin-Helmholtz instability. *J. Fluid Mech*, 6 (4):583–598, 1959b. URL https://doi.org/10.1017/S0022112059000842.

Miles, J. W. On the generation of surface waves by shear flows. part 4. *J. Fluid Mech*, 13 (3):433–448, 1962. URL https://doi.org/10.1017/S0022112062000828.

Müller, M., Homleid, M., Ivarsson, K.-I., Køltzow, M. A., Lindskog, M., Midtbø, K. H., Andrae, U., Aspelien, T., Berggren, L., Bjørge, D., et al. AROME-MetCoOp: A Nordic convective-scale operational weather prediction model. *Weather and Forecasting*, 32 (2):609–627, 2017. URL https://doi.org/10.1175/WAF-D-16-0099.1.

Newman, J. N. *Marine hydrodynamics* (The MIT press, 2018). URL https://mitpress.mit.edu/9780262534826/marine-hydrodynamics/.

Ochi, M. K. and Hubble, E. N. Six-parameter wave spectra. *Coastal Engineering Proceedings*, 1 (15):17, 1976. URL https://doi.org/10.9753/icce.v15.17.

Pasquill, F. The estimation of the dispersion of windborne material. *Meteorological Magazine*, 90:33–49, 1961. URL https://digital.nmla.metoffice.gov.uk/download/file/sdb%3AdigitalFile%7Cd75249c9-59ed-41cd-9eb0-1ba3176e7b36.

Pasquill, F. Atmospheric dispersion modeling. *Journal of the Air Pollution Control Association*, 29 (2):117–119, 1979. URL https://doi.org/10.1080/00022470.1979.10470764.

Pasquill, F. and Smith, F. B. *Atmospheric diffusion* (Ellis Horwood Ltd., 1983). URL https://www.osti.gov/servlets/purl/5591108.

Pierson Jr, W. J. and Moskowitz, L. A proposed spectral form for fully developed wind seas based on the similarity theory of S. A. Kitaigorodskii. *Journal of geophysical research*, 69 (24):5181–5190, 1964. URL https://doi.org/10.1029/JZ069i024p05181.

Pope, S. B. *Turbulent flows* (Cambridge university press, 2000). URL https://doi.org/10.1017/CBO9780511840531.

Reistad, M., Breivik, Ø., Haakenstad, H., Aarnes, O. J., Furevik, B. R., and Bidlot, J.-R. A high-resolution hindcast of wind and waves for the North Sea, the Norwegian Sea, and the Barents Sea. *Journal of Geophysical Research: Oceans*, 116 (C5), 2011. URL https://doi.org/10.1029/2010JC006402.

Sagaut, P. and Lee, Y.-T. Large eddy simulation for incompressible flows: An introduction. scientific computation series. *Appl. Mech. Rev.*, 55 (6):B115–B116, 2002. URL https://doi.org/10.1007/b137536.

Saltbones, J., Foss, A., and Bartnicki, J. Severe nuclear accident program (SNAP) a real time dispersion model. In *Air Pollution Modeling and Its Application XI*, pp. 471–479 (Springer, 1996). URL https://doi.org/10.1007/978-1-4615-5841-5_50.

Saltbones, J., Foss, A., and Bartnicki, J. Norwegian meteorological institute's real-time dispersion model SNAP (severe nuclear accident program): Runs for ETEX and ATMES II experiments with different meteorological input. *Atmospheric Environment*, 32 (24):4277–4283, 1998. URL https://doi.org/10.1016/S1352-2310(98)00192-7.

Schwarzkopf, J. D., Sommerfeld, M., Crowe, C. T., and Tsuji, Y. *Multiphase flows with droplets and particles* (CRC press, Taylor & Francis Group, Boca Raton, Florida, U.S., 2012). URL https://doi.org/10.1201/b11103.

Seity, Y., Brousseau, P., Malardel, S., Hello, G., Bénard, P., Bouttier, F., Lac, C., and Masson, V. The AROME-France convective-scale operational model. *Monthly Weather Review*, 139 (3):976–991, 2011. URL https://doi.org/10.1175/2010MWR3425.1.

Semedo, A., Sušelj, K., Rutgersson, A., and Sterl, A. A global view on the wind sea and swell climate and variability from ERA-40. *Journal of Climate*, 24 (5):1461–1479, 2011. URL https://doi.org/10.1175/2010JCLI3718.1.

Semedo, A., Vettor, R., Breivik, Ø., Sterl, A., Reistad, M., Soares, C. G., and Lima, D. The wind sea and swell waves climate in the nordic seas. *Ocean dynamics*, 65:223–240, 2015. URL https://doi.org/10.1007/s10236-014-0788-4.

Sempreviva, A. M. and Gryning, S.-E. Mixing height over water and its role on the correlation between temperature and humidity fluctuations in the unstable surface layer. *Boundary-layer meteorology*, 97 (2):273–291, 2000. URL https://doi.org/10.1023/A:1002749729856.

Skamarock, W. C., Klemp, J. B., Dudhia, J., Gill, D. O., Liu, Z., Berner, J., Wang, W., Powers, J. G., Duda, M. G., Barker, D. M., et al. A description of the advanced research wrf model version 4. *National Center for Atmospheric Research: Boulder, CO, USA*, 145 (145):550, 2019. URL http://dx.doi.org/10.5065/1dfh-6p97.

Soares, C. G. Representation of double-peaked sea wave spectra. *Ocean Engineering*, 11 (2):185–207, 1984. URL https://doi.org/10.1016/0029-8018(84)90019-2.

Stockie, J. M. The mathematics of atmospheric dispersion modeling. *Siam Review*, 53 (2):349–372, 2011. URL https://doi.org/10.1137/10080991X.

Stull, R. B. *An introduction to boundary layer meteorology*, vol. 13 (Springer Science & Business Media, 1988). URL https://doi.org/10.1007/978-94-009-3027-8.

Sullivan, P. P., Edson, J. B., Hristov, T., and McWilliams, J. C. Large-eddy simulations and observations of atmospheric marine boundary layers above nonequillibrium surface waves. *J. Atmos. Sci.*, 65:1225–1245, 2008. URL https://doi.org/10.1175/2007JAS2427.1.

Sullivan, P. P. and McWilliams, J. C. Turbulent flow over water waves in the presence of stratification. *Physics of Fluids*, 14 (3):1182–1195, 2002. URL https://doi.org/10.1063/1.1447915.

Sullivan, P. P. and McWilliams, J. C. Dynamics of winds and currents coupled to surface waves. *Annu. Rev. Fluid Mech*, 42:19–42, 2010. URL https://doi.org/10.1146/annurev-fluid-121108-145541.

Sullivan, P. P., McWilliams, J. C., and Moeng, C.-H. Simulation of turbulent flow over idealized waves. *J. Fluid Mech*, 404:47–85, 2000. URL https://doi.org/10.1017/S0022112099006965.

Sullivan, P. P., McWilliams, J. C., and Patton, E. G. Large-eddy simulation of marine atmospheric boundary layers above a spectrum of moving waves. *J. Atmos. Sci.*, 71:4001–4027, 2014. URL https://doi.org/10.1175/JAS-D-14-0095.1.

Taylor, G. I. Diffusion by continuous movements. *Proc. Lond. Math. Soc.*, 2 (1):196–212, 1922. URL https://doi.org/10.1112/plms/s2-20.1.196.

Thykier-Nielsen, S., Deme, S., and Mikkelsen, T. Description of the atmospheric dispersion module rimpuff. *Riso National Laboratory, PO Box*, 49, 1999. URL https://www.researchgate.net/publication/228741276_Description_of_the_atmospheric_dispersion_module_RIMPUFF.

Torsethaugen, K. A two peak wave spectrum model. *Proceeding OMAE Glasgow*, 1993. URL https://www.researchgate.net/publication/280689204_Two_peak_wave_spectrum_model.

Turner, D. B. *Workbook of atmospheric dispersion estimates: an introduction to dispersion modeling* (CRC press, 1994). URL https://nepis.epa.gov/Exe/ZyPURL.cgi?Dockey=9100JEIO.TXT.

Van Duin, C. A. and Janssen, P. A. E. M. An analytic model of the generation of surface gravity waves by turbulent air flow. *J. Fluid Mech*, 236:197–215, 1992. URL https://doi.org/10.1017/S0022112092001393.

Versteeg, H. K. and Malalasekera, W. *An introduction to computational fluid dynamics: the finite volume method* (Pearson education, 2007).

Warner, T. T. *Numerical weather and climate prediction* (Cambridge University Press, 2010). URL https://doi.org/10.1017/CBO9780511763243.

West, B. J., Brueckner, K. A., Janda, R. S., Milder, D. M., and Milton, R. L. A new numerical method for surface hydrodynamics. *Journal of Geophysical Research: Oceans*, 92 (C11):11803–11824, 1987. URL https://doi.org/10.1029/JC092iC11p11803.

Yang, D., Meneveau, C., and Shen, L. Dynamic modelling of sea-surface roughness for large-eddy simulation of wind over ocean wavefield. *J. Fluid Mech*, 726:62–99, 2013. URL https://doi.org/10.1017/jfm.2013.215.

Yang, D. and Shen, L. Characteristics of coherent vortical structures in turbulent flows over progressive waves. *Phys. Fluids*, 21:125106, 2009. URL https://doi.org/10.1063/1.3275851.

Yang, D. and Shen, L. Direct-simulation-based study of turbulent flow over various waving boundaries. *J. Fluid Mech*, 650:131–180, 2010. URL https://doi.org/10.1017/S0022112009993557.

Yang, D. and Shen, L. Direct numerical simulation of scalar transport in turbulent flows over progressive surface waves. *J. Fluid Mech*, 819:58–103, 2017. URL https://doi.org/10.1017/jfm.2017.164.

Zakharov, V. E. Stability of periodic waves of finite amplitude on the surface of a deep fluid. *Journal of Applied Mechanics and Technical Physics*, 9 (2):190–194, 1968. URL https://doi.org/10.1007/BF00913182.

About FFI

The Norwegian Defence Research Establishment (FFI) was founded 11th of April 1946. It is organised as an administrative agency subordinate to the Ministry of Defence.

FFI's mission

FFI is the prime institution responsible for defence related research in Norway. Its principal mission is to carry out research and development to meet the requirements of the Armed Forces. FFI has the role of chief adviser to the political and military leadership. In particular, the institute shall focus on aspects of the development in science and technology that can influence our security policy or defence planning.

FFI's vision

FFI turns knowledge and ideas into an efficient defence.

FFI's characteristics

Creative, daring, broad-minded and responsible.

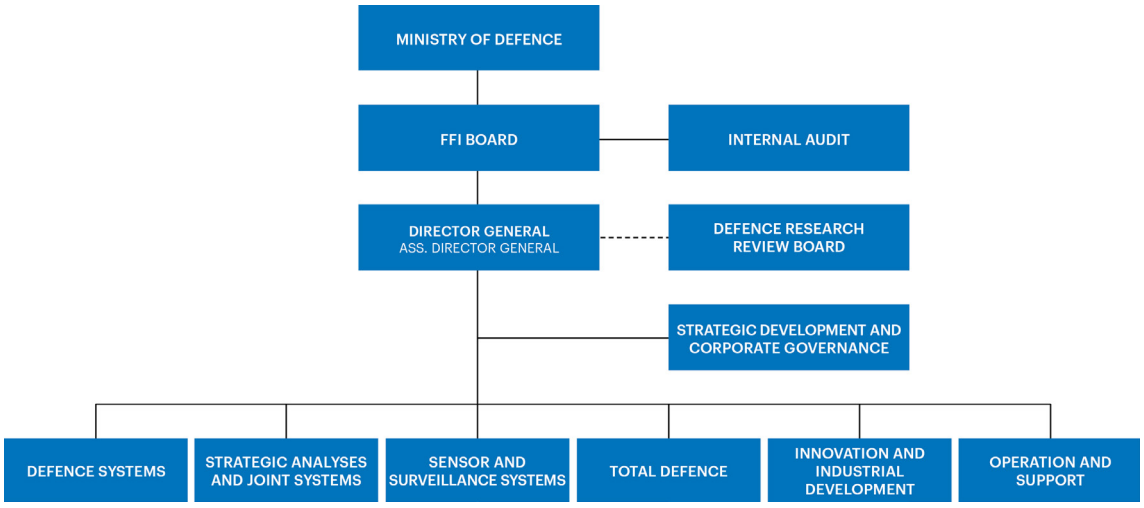

Forsvarets forskningsinstitutt (FFI)
Postboks 25
2027 Kjeller

Besøksadresse:
Kjeller: Instituttveien 20, Kjeller
Horten: Nedre vei 16, Karljohansvern, Horten

Telefon: 91 50 30 03
E-post: post@ffi.no
ffi.no

Norwegian Defence Research Establishment (FFI)
PO box 25
NO-2027 Kjeller
NORWAY

Visitor address:
Kjeller: Instituttveien 20, Kjeller
Horten: Nedre vei 16, Karljohansvern, Horten

Telephone: +47 91 50 30 03
E-mail: post@ffi.no
ffi.no/en